Matériaux cellulaires architecturés et biosourcés, obtenus par solidification d'hydrogels de nanofibres de cellulose

Florian Martoïa[1], Pierre Dumont[1], Laurent Orgéas[2], Elodie Boller[3]

(1) LaMCoS (CNRS/INSA-Lyon/Univ. Lyon)
(2) 3SR Lab. (CNRS/Grenoble INP/Univ. Grenoble Alpes)
(3) ESRF –The European Synchrotron, Grenoble,

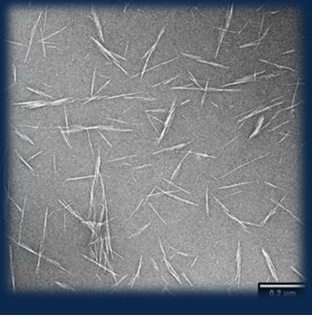

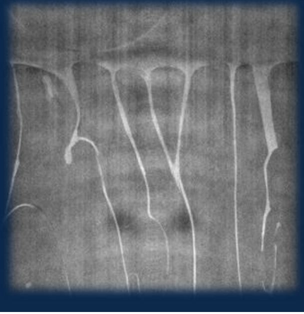

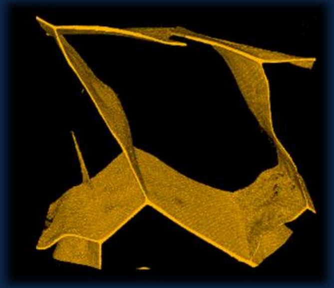

Nanocelluloses: Cellulose nanofibrils (CNFs) and cellulose nanocrystals (CNCs)

Paper pulp

Wood fibres

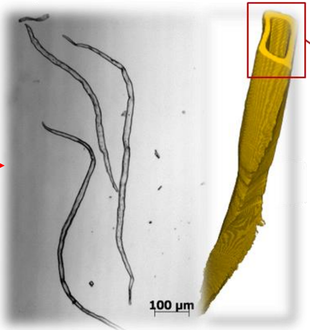

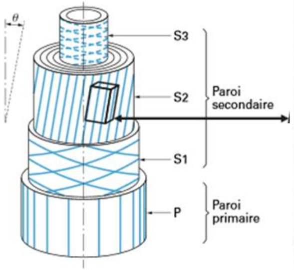

[Toungara et al., 2015]

Fibre cell wall

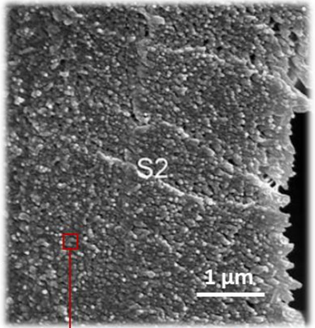

[Donaldson et al., Wood Sci. Technol., 2007]

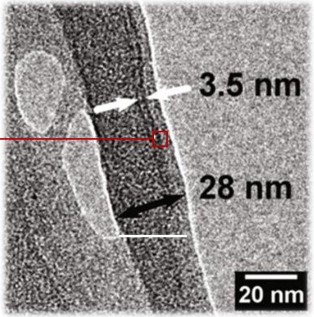

Bundles of cellulose fibrils

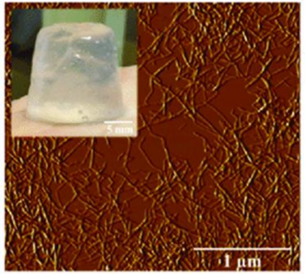

Cellulose nanofibrils (CNFs)

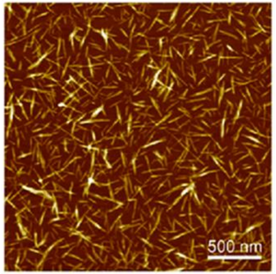

Cellulose nanocrystals (CNCs)

- CNFs and CNCs are extracted in the form of hydrogels
- Slender biobased nanofibres $10 \leq \frac{l}{d} \leq 300$
- Oustanding intrinsic mechanical properties $(E_\mathrm{L} \sim 100 - 200\ \mathrm{GPa})$

Potential applications of CNFs and CNCs

Hydrogels & Additives

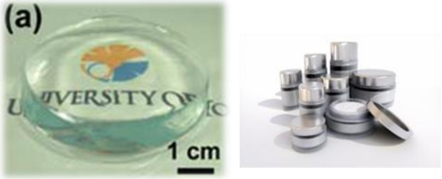

[Saito et al., Soft Matter. 2011]

Fibrous Suspensions

- Packaging
- Energy
- **Structural materials**
- Biomedical
- Healthcare
- Filtration
- Electronics

Foams

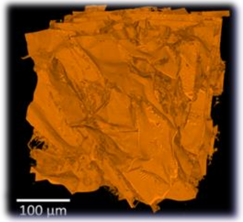

[Martoïa et al., Materials & Design, 2016]

Continuous filaments & fabrics

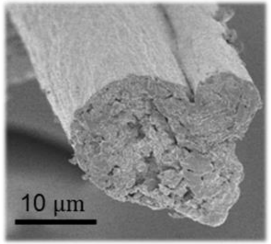

[Hakansson et al., Nature Comm. 2014]

Films & Nanopapers

[Larsson et al., Biomacromolecules 2014]
[Fukuzumi, Biomacromolecules 2011, 2013]

Composites

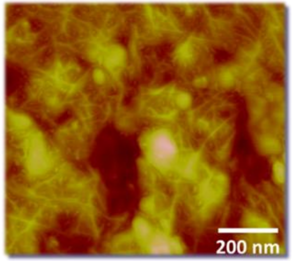

[Martoïa et al., RSC Advances, 2016]

Ice-templated nanocellulose foams

Basis of ice-templating

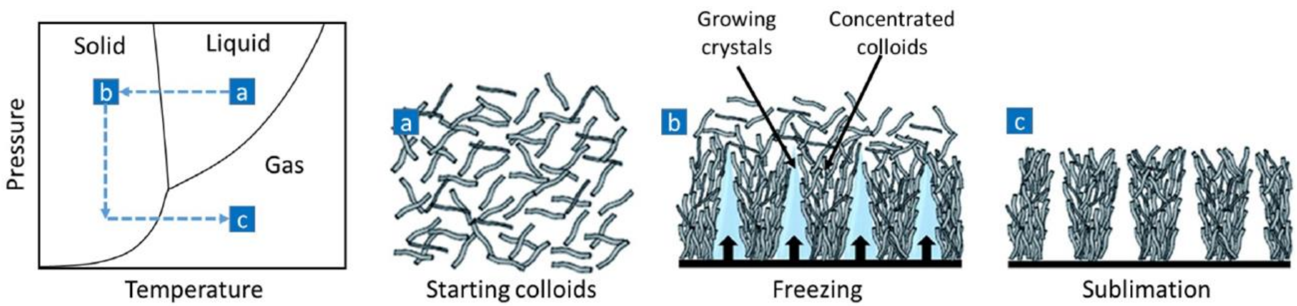

[Lavoine et al. JMCA, 2017]

CNC/CNF hydrogel

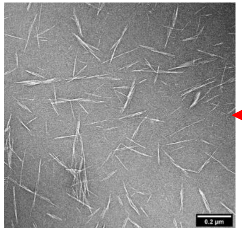

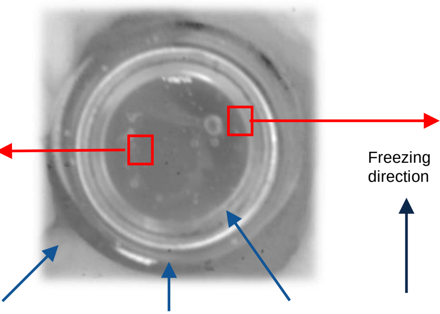

Ice bath Glass tube Ice front

Ice-crystal growth

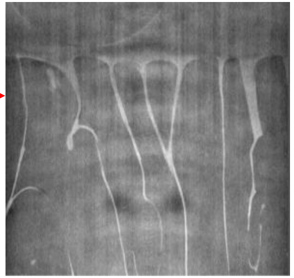

Freeze-dried CNC/CNF foam

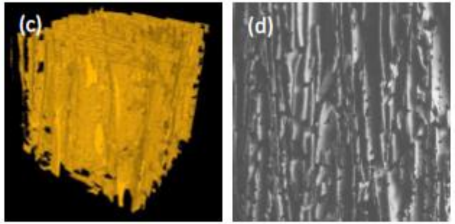

Nanocellulose foams: promising biobased cellular materials for structural applications?

Typical compression response of nanocellulose foams

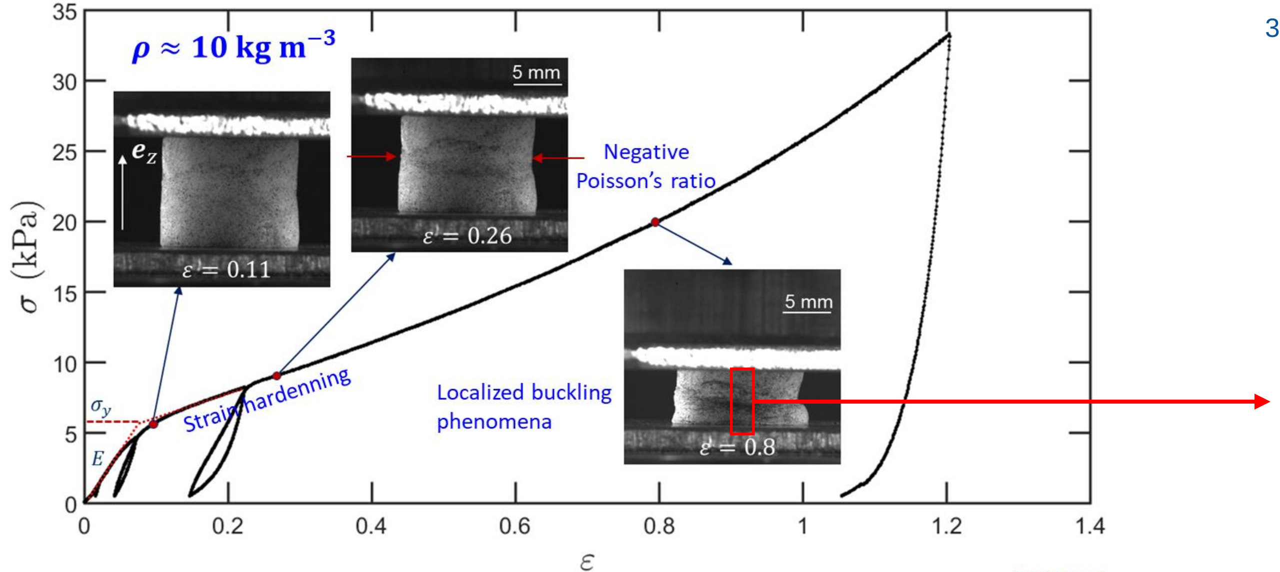

[Martoïa et al., Materials & Design, 2016]

3D observations during in-situ compression

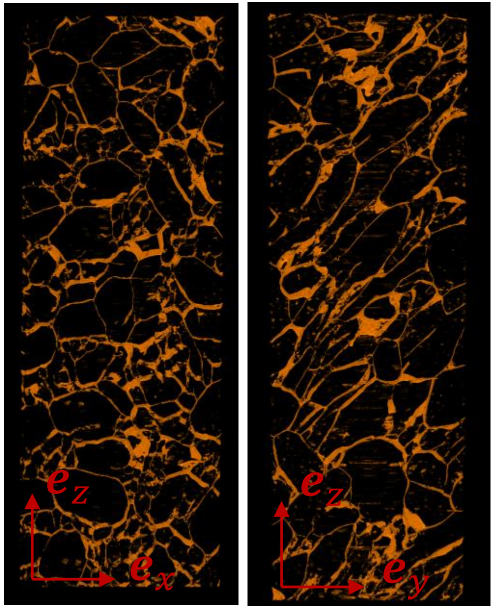

ID19 beamline, ESRF, voxel size: 0.32^3 µm^3

- Elasto-plastic behaviour with marked consolidation
- Large ductility and auxetic behaviour
- Promising use as shock absorber materials

Nanocellulose foams: promising biobased cellular materials for structural applications?

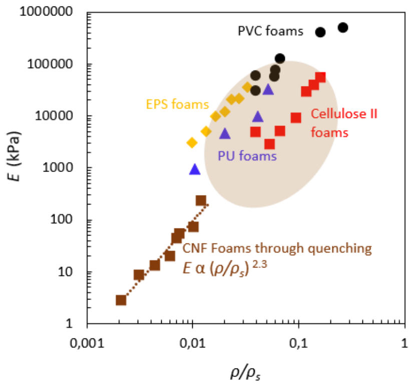

[Ashby and Gibson, 1999]
[Sehaqui et al., Soft Matter 2010]]
[Sescousse et al., Carbohydr. Polym., 2011]

Foam cell wall = nanopaper
E_s = 10-15 GPa!

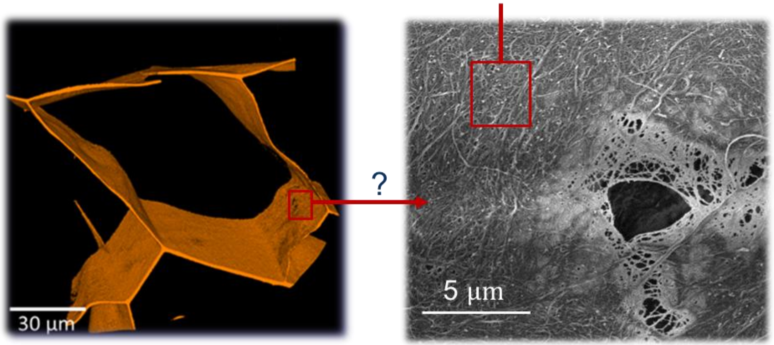

$$E = \mathcal{F}(E_s, \rho_s, \rho, \text{cell and cell wall geometry})$$

$$\left(\frac{E_s}{\rho_s}\right)_{cellulose} > \left(\frac{E_s}{\rho_s}\right)_{polymer}$$

- ➢ Limited range of densities ($\rho < 150$ kg m^{-3})
- ➢ Lower mechanical properties than most of classical polymer foams

→ Better understanding of process-induced foam microstructures!

Motivations and objectives

- **Better understanding of process-induced foam microstructures!**

1. **Prepare homogeneous hydrogels with high concentrations of cellulose nanofibres!**

2. **Characterise the forming of ice-templated foams**

    - **Effect of the nanofibre aspect ratio: CNFs vs CNCs**
    - **Effect of the nanofibre content**

3. **Assess the mechanical performances of ice-templated foams**

Materials

Cellulose nanofibrils (CNFs) and Cellulose nanocrystals (CNCs)

- TEMPO-oxidised **CNFs** supplied by the Centre Technique du papier
  - Initial hydrogel concentration c = 1.2 wt%
  - Content of carboxyl groups: 1.5 mmol g^{-1}

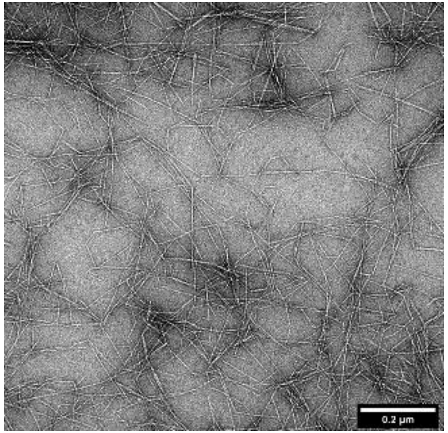

$\bar{d} = 7$ nm and $\bar{l}\ \alpha$ 1200 nm

$r = \bar{l}/\bar{d} \approx 300$

- **CNCs** supplied by CelluForce (Canada)
  - Spray-dried powder
  - Content of sulfate half ester groups: 0.25 mmol g^{-1}

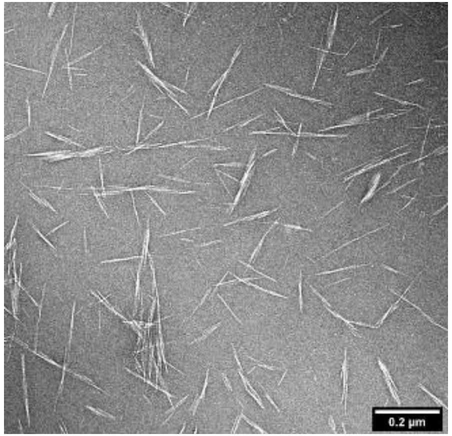

$\bar{d} = 12$ nm and $\bar{l}\ \alpha$ 150 nm

$r = \bar{l}/\bar{d} \approx 12$

➢ Electrostatically stabilised hydrogels

Materials

Preparation of concentrated and highly concentrated CNF and CNC hydrogels

- TEMPO-oxidised CNF hydrogels
  - Concentration procedure$^{(*)}$: mechanical stirring under vaccum at T = 60°C

(*) Martoïa et al. Carbohydrate Polymers, 2022

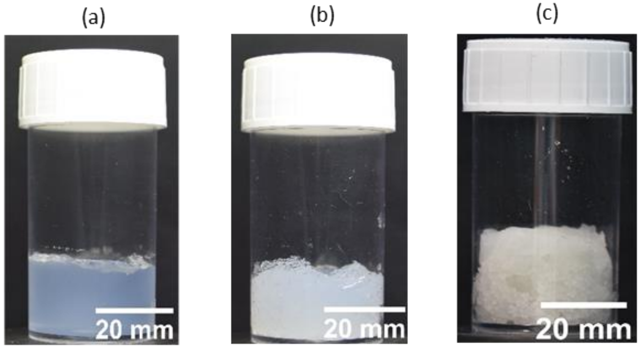

(a) 1.2 wt.% (ϕ_f = 0.8%), (b) 2 wt.% (ϕ_f = 1.4%), (c) 8.6 wt.% (ϕ_f = 5.9%)

- CNC hydrogels
  - Mechanical stirring at high velocity (12000 rpm)$^{(*)}$ at ambiant température

(*) Martoïa et al. Carbohydrate Polymers, 2022

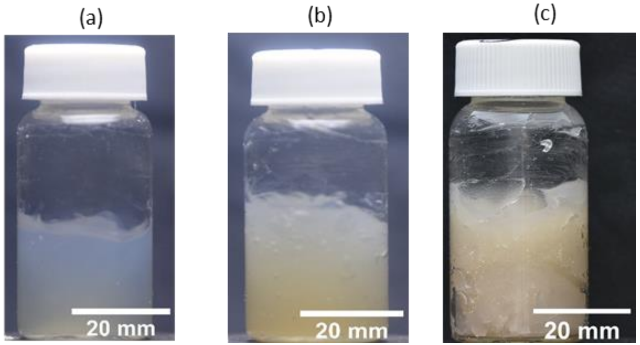

(a) 6.5 wt.% (ϕ_f = 4.4%), (b) 10 wt.% (ϕ_f= 6.9%), (c) 24.5 wt.% (ϕ_f = 17.9%).

➢ **Average nanofibre-nanofibre contacts$^{(*)}$ per nanofibre $\bar{z} \gg 2$→ highly concentrated regime!**

(*) Toll, J. Rheol. 1993

Characterisation of the forming of ice-templated foams

In situ unidirectionnal solidification experiments during synchrotron X-ray microtomography

Solidification setup installed on the ID19 beamline at ESRF

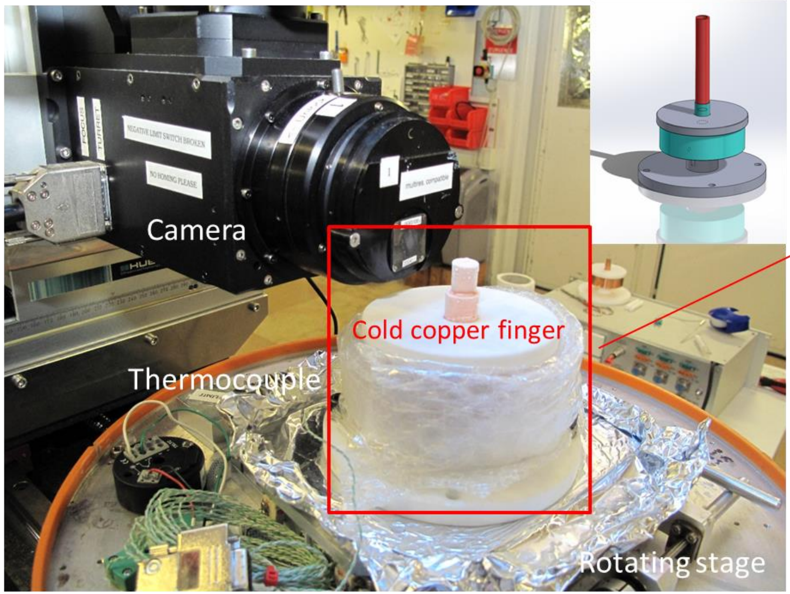

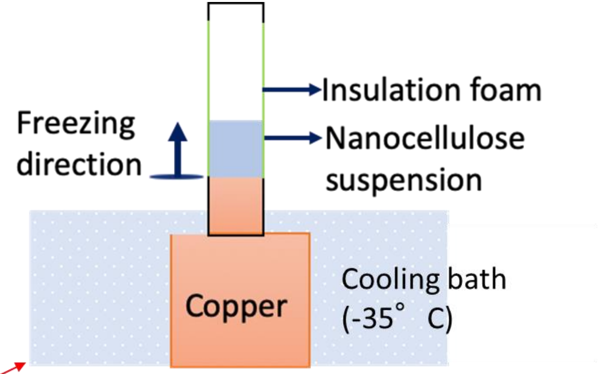

High resolution and real-time X-ray microtomography:

- X-ray energy 19 keV
- Voxel size: 0.55^3 μm^3
- 2000 X-ray radiographs
- ROI 1008 × 1008 pixels
- Scanning time ≈ 1 s

Characterisation of the forming of ice-templated foams

In situ unidirectionnal solidification experiments during synchrotron X-ray microtomography

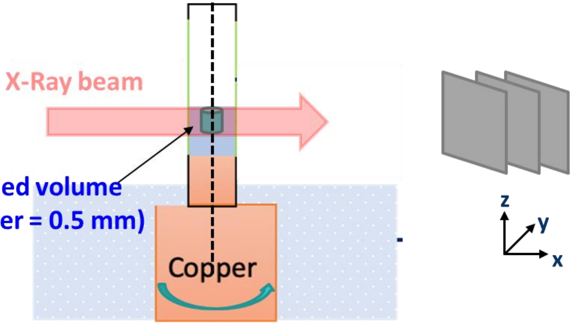

Scanned volume (diameter = 0.5 mm)

Rotation axis

X-ray radiographs obtained for various angular positions

X-ray radiographs

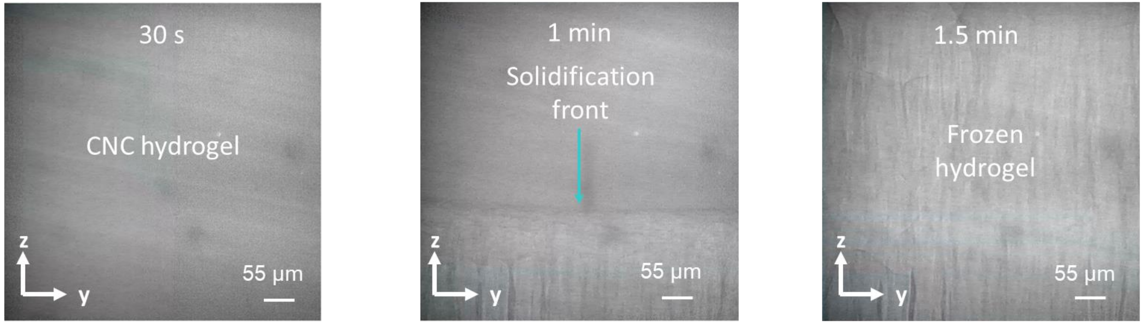

Characterisation of the forming of ice-templated foams

In situ undirectionnal solidification experiments during synchrotron X-ray microtomography

- CNC hydrogel (9 wt%)

Cross section (yz plane)

cell walls (CNC + water)

Freezing direction

Ice phase

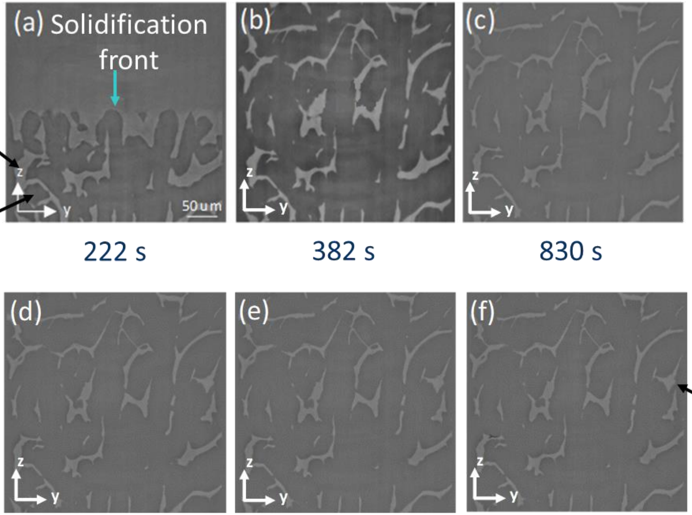

222 s | 382 s | 830 s

926 s | 990 s | 1086 s

cell walls (CNC)

CNC phase at the end of the solidification

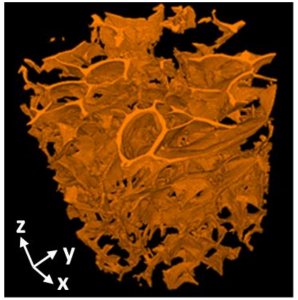

$400 \times 400 \times 560\ \mu m^3$

- ➢ Growth of ice crystals along the vertical direction
- ➢ Longitudinal ice growth rate $V_{\parallel} \sim 1\ \mu m\ s^{-1}$

Characterisation of the forming of ice-templated foams

In situ undirectionnal solidification experiments during synchrotron X-ray microtomography

- CNC hydrogel (9 wt%)

Cross section (xy plane) :

Cell walls :
CNC hydrogels in hyperconcentrated regimes!!!

Ice phase

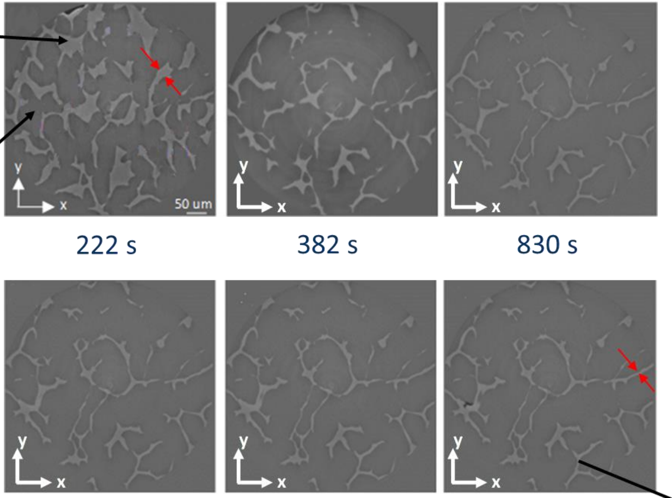

222 s 382 s 830 s

926 s 990 s 1086 s

cell walls (CNC)

CNC phase at the end of the solidification phase

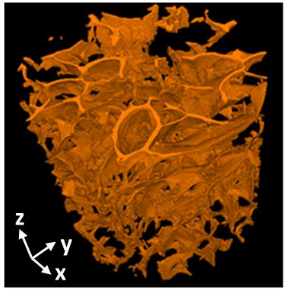

$400 \times 400 \times 560\ \mu\mathrm{m}^3$

- Reduction of cell walls thickness → lateral growth of ice crystals
- Lateral ice growth rate $V_\perp \sim 7 \times 10^{-3}\ \mu\mathrm{m.s}^{-1}$
- Squezzing and (progressive) consolidation mechanisms of CNC hydrogel

Characterisation of the forming of ice-templated foams

Effect of the nanofibre aspect ratio and content

Lamellar structures

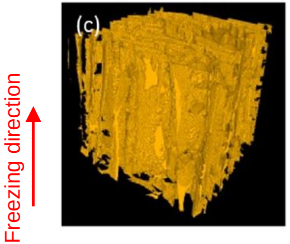

“Isotropic” porous structures

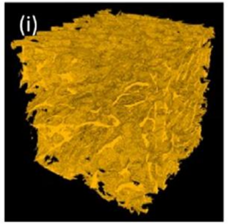

Degree of anisotropy

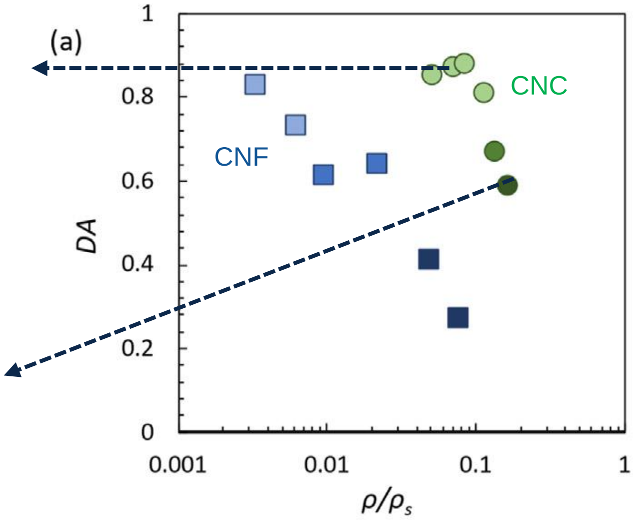

Mean pore thickness

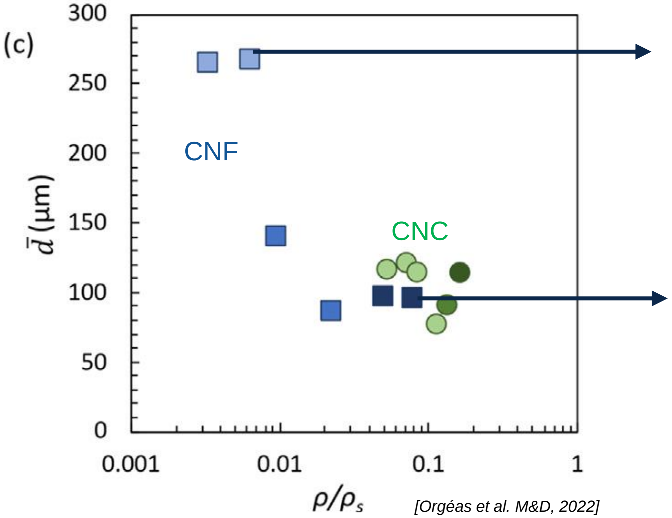

[Orgéas et al. M&D, 2022]

Columnar structures

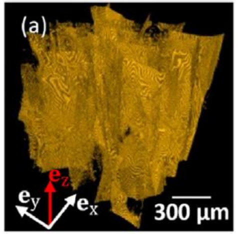

“Isotropic” porous structures

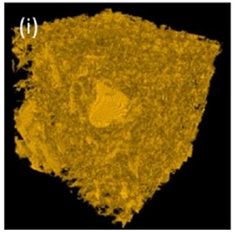

- → Drastic effect of the nanofibre aspect ratio on the foam microstructure
- → Microstructures of foams switch from anisotropy to isotropy while increasing the nanofibre concentration or aspect ratio.
- → Crucial role of the rheology (restrain ice-crystal growth + promote ice-crystal nucleation)

Ice-templating of highly concentrated nanofibre hydrogels

Mechanical properties: effect of the relative density and aspect ratio of cellulose nanofibres

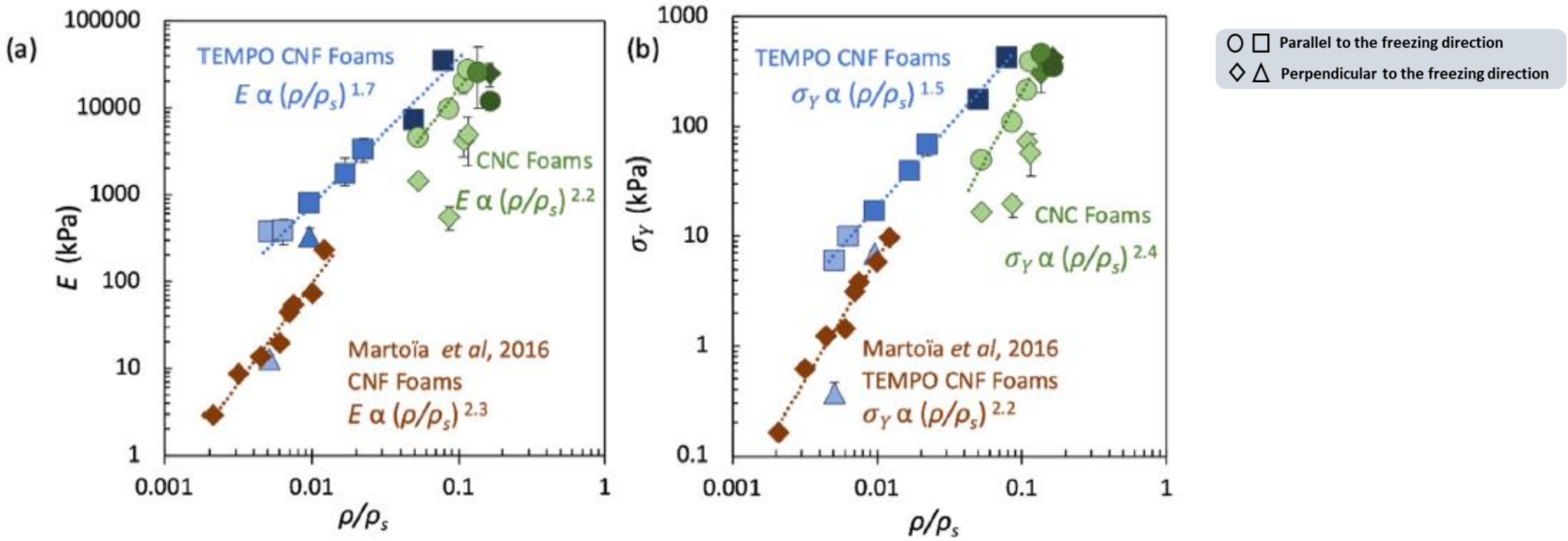

- → Pronounced mechanical anisotropy
- → Increasing the nanofibre content and aspect ratio leads to substantial improvement of the foam stiffness E and yield strength σ_Y

Ice-templating of highly concentrated nanofibre hydrogels

Mechanical properties: effect of the relative density and aspect ratio of cellulose nanofibres

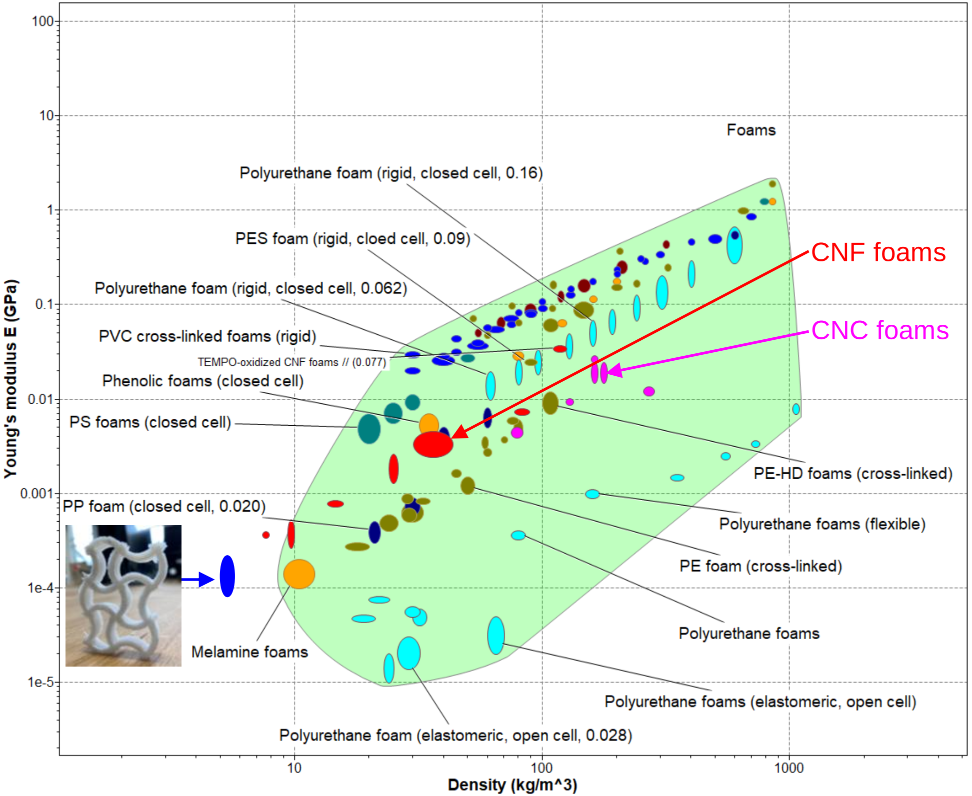

→ These biobased materials exhibit mechanical properties that are comparable with rigid commercially-available polymer foams

→ CNF foams exhibit interesting specific mechanical properties for lightweight structural applications.

Ice-templating of highly concentrated nanofibre hydrogels

Mechanical properties: effect of the relative density and aspect ratio of cellulose nanofibres

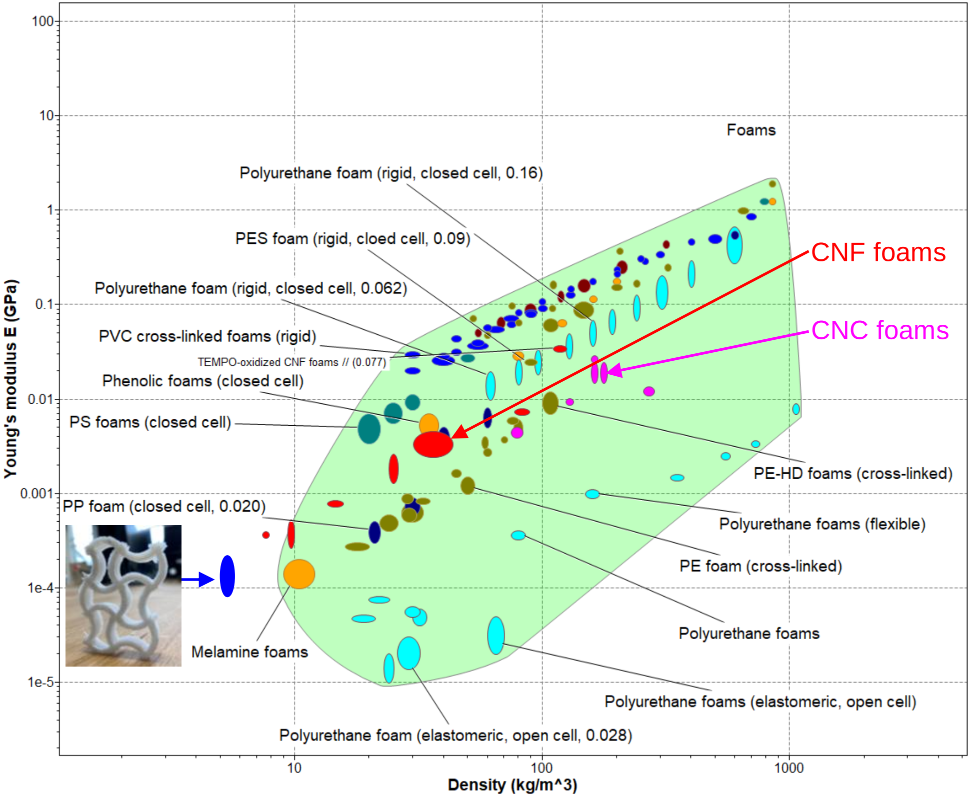

- → These biobased materials exhibit mechanical properties that are comparable with rigid commercially-available polymer foams
- → CNF foams exhibit interesting specific mechanical properties for lightweight structural applications.

→ Bimodal foams: mechanical stirring during freezing

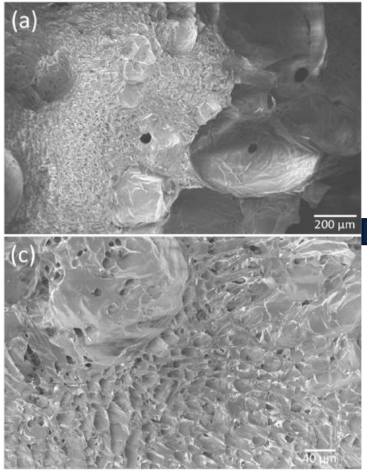

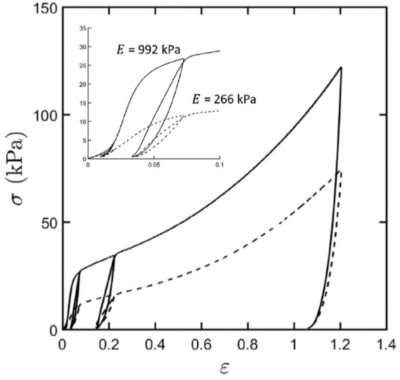

Ice-templating of highly concentrated nanofibre hydrogels

Mechanical properties: effect of the relative density and aspect ratio of cellulose nanofibres

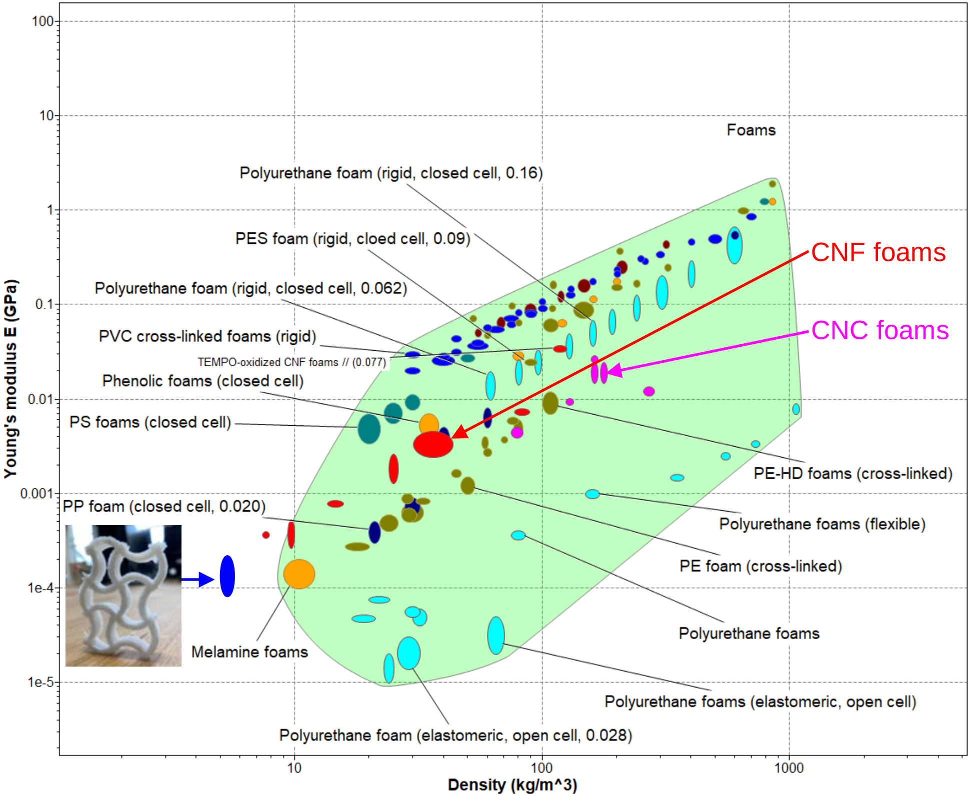

→ These biobased materials exhibit mechanical properties that are comparable with rigid commercially-available polymer foams

→ CNF foams exhibit interesting specific mechanical properties for lightweight structural applications.

→ Mold design → foams with two-scale pore structure

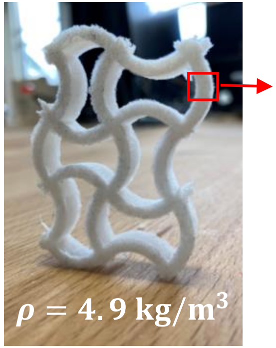

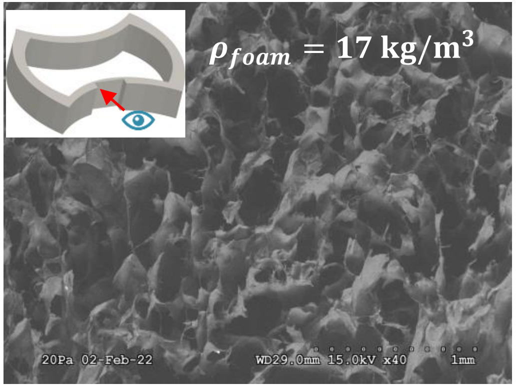

Merci de votre écoute !

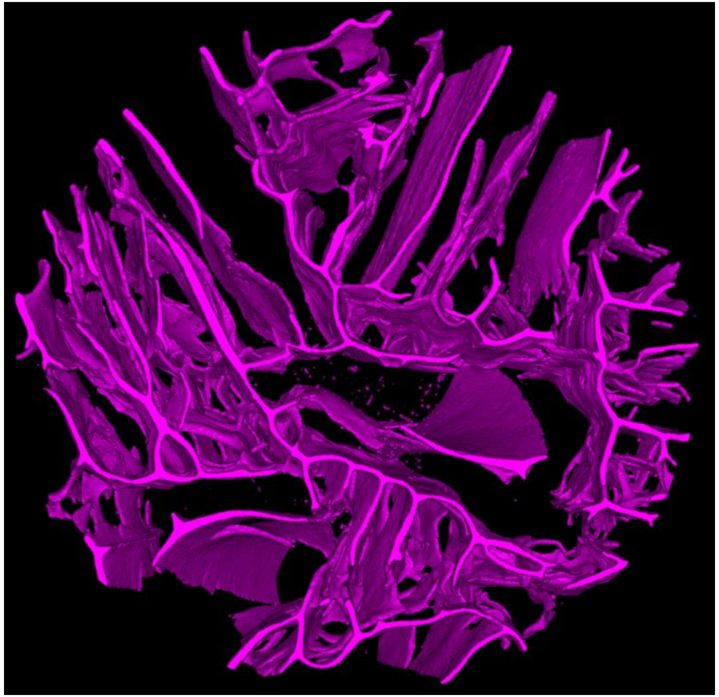

Articles relatifs à ces travaux :

Martoïa et al., M&D (2016)

Orgéas et al. M&D (2023)

Dumont et al. Carb. Polym. (2023)

Elongational rheology of concentrated hydrogels

Lubricated compression experiments on cylindrical samples

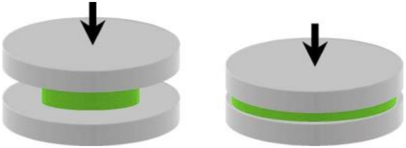

Lubricated plate surfaces with silicone oil ($\mu = 0.02$ Pa s)

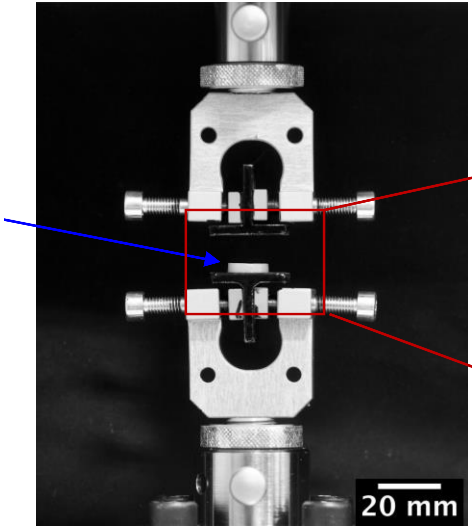

- Electromechanical testing machine equipped with parallel plates

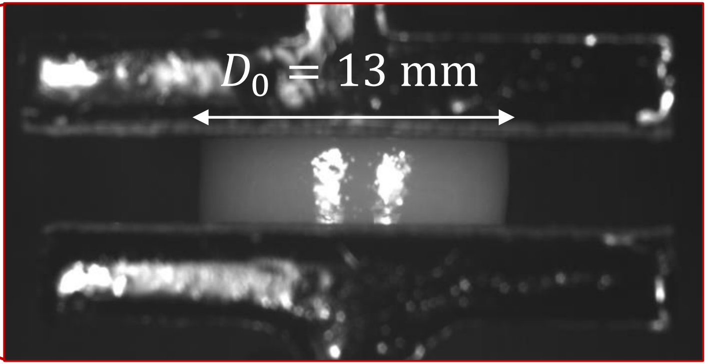

- Cylindrical samples: diameter $D_0 = 13$ mm and height $h_0 = 3$ mm
- Constant compression velocity v_0: 0.2 to 150 mm min^{-1}
- Monotonic and cyclic load-unload compression tests

[Martoïa et al. *Carbohydrate Polymers*, 2022]
[Dumont et al. *Carbohydrate Polymers*, 2022]

Elongational rheology of concentrated hydrogels

Lubricated compression experiments on cylindrical samples: effect of the strain rate

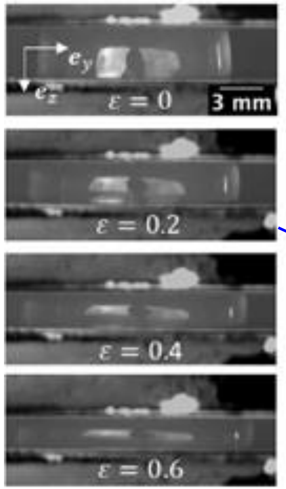

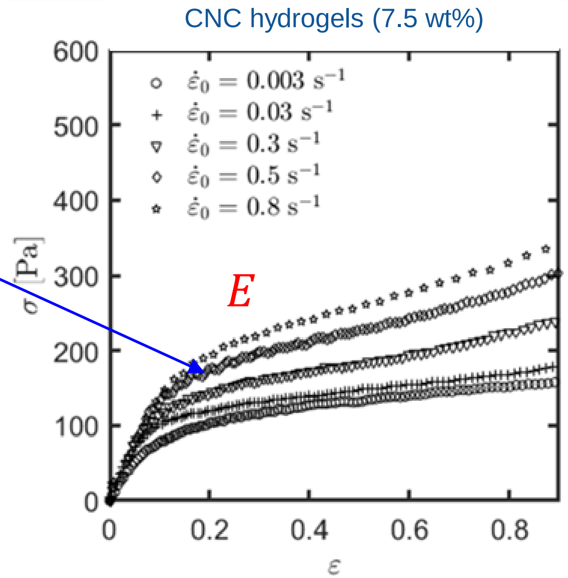

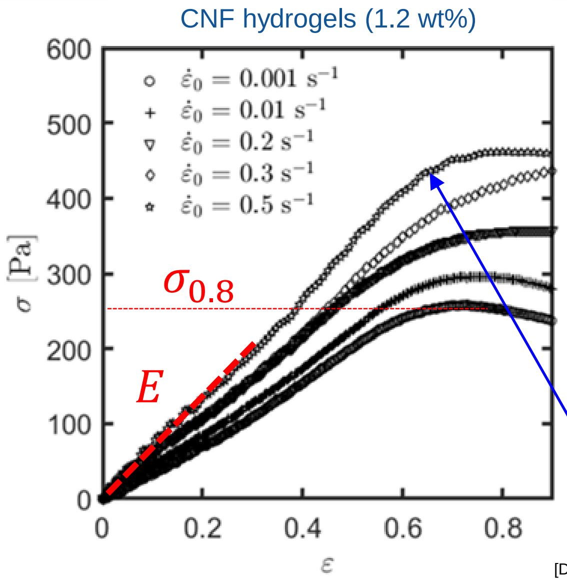

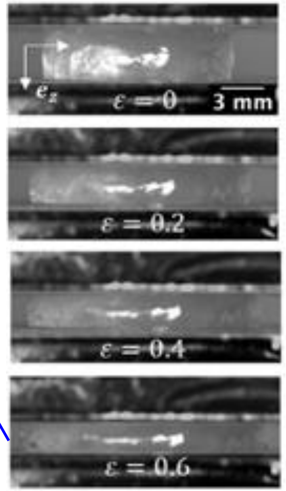

[Dumont et al. *Carbohydrate Polymers*, 2022]

→ Regarless of the strain-rates: homogeneous one-phase flow behaviour!
→ Elasto-viscoplastic behaviour typical of many soft-glassy materials

→ TEMPO-oxidised CNF hygrogels exhibited higher elastic and plastic properties compared with CNC hydrogels → Effect of the nanofibre aspect ratio!

Elongational rheology of concentrated hydrogels

Lubricated compression experiments on cylindrical samples: effect of the nanofibre content and aspect ratio

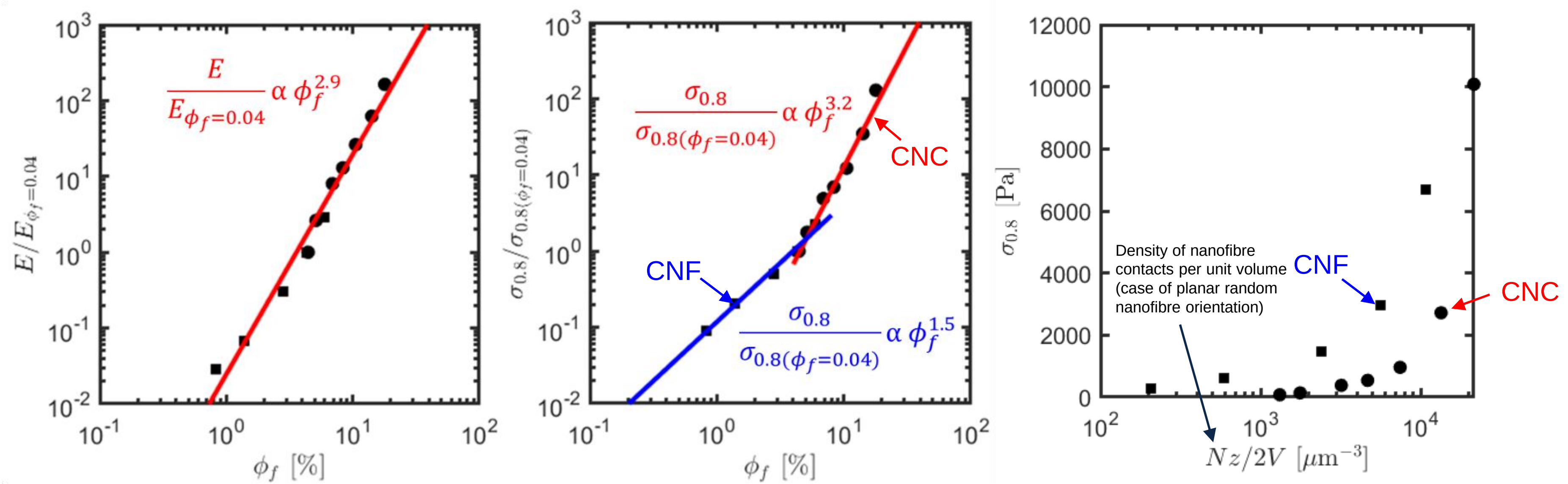

[Dumont et al. *Carbohydrate Polymers*, 2022]

→ Power-law dependance of E and $\sigma_{0.8}$ with the hydrogel concentration
→ Effect of nanofibre content and aspect ratio
→ Flow stress is not uniquely related to nanofibre entanglement (role of colloidal interactions?)

Ice-templating of highly concentrated nanofibre hydrogels

Fabrication of foams

Unidirectional solidification setup

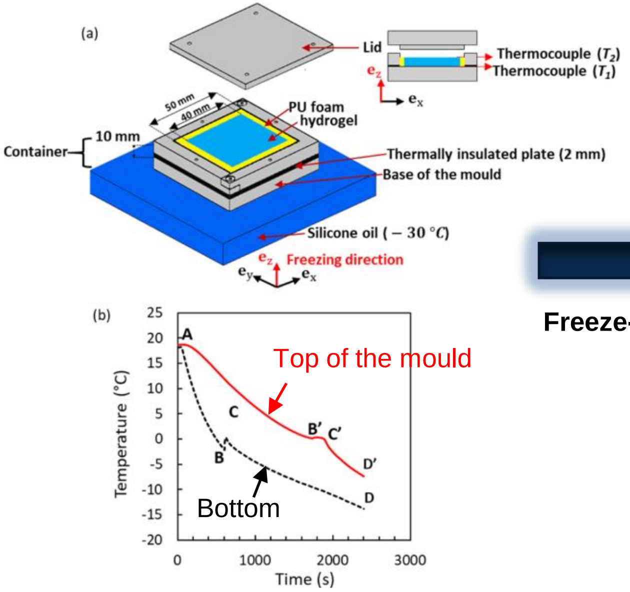

Freeze-drying

Square plates of foams (40×40×10 mm^3)

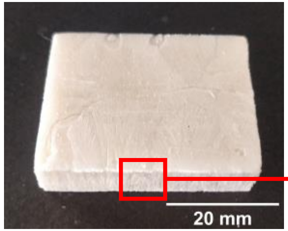

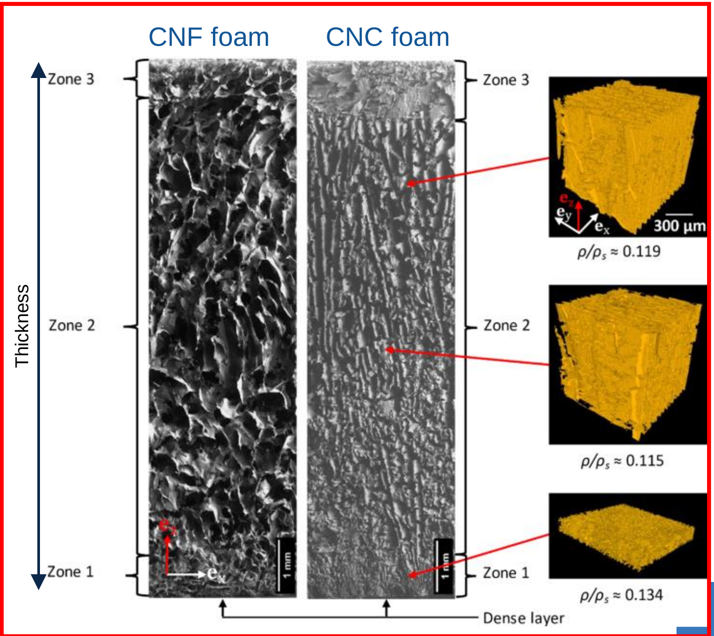

→ Two solidification fronts initiated from the bottom (points B-C) and the top (points B'-C') of the mould
→ Produced foams systematically exhibit 3 distinct zones in their microstructure